

# Nickel and Nickel–Magnesia Catalysts Active in the Hydrogenation of 1,4-Butanedinitrile

Marc Serra,\* Pilar Salagre,\*<sup>1</sup> Yolanda Cesteros,\* Francisco Medina,† and Jesús E. Sueiras†

\**Facultat de Química, Universitat Rovira i Virgili, Pl. Imperial Tarraco, 1, 43005, Tarragona, Spain; and †Escola Tècnica Superior d'Enginyeria Química, Universitat Rovira i Virgili, Pl. Imperial Tarraco, 1, 43005, Tarragona, Spain*

Received July 28, 2000; revised September 28, 2000; accepted September 28, 2000

Several NiO–MgO systems were synthesized to be studied as nickel catalysts for the hydrogenation of 1,4-butanedinitrile in the gas phase and compared with a bulk NiO of controlled morphology. All samples were characterized by XRD, BET, TPR, TPD, SEM, and H<sub>2</sub> chemisorption techniques. The Ni–MgO systems had higher activities than the Ni bulk catalyst. The most active catalyst at all reaction temperatures was type R4C<sub>B</sub> which had homogeneous particles of about 1000 Å, the highest metal surface area, and the highest coverage with weakly bound hydrogen. The presence of basic magnesia suppresses the condensation reactions and consequently favors the elimination of amines, and prevents catalyst deactivation. The selectivity toward the different products not only depends on the catalytic properties but can also be modified by controlling the hydrogen/dinitrile ratio. The highest selectivity to 4-aminobutanenitrile was achieved by catalyst R4C<sub>B</sub>, with 85% at 100% conversion and working at a space velocity of 13,000 h<sup>-1</sup> and 343 K. This selectivity could be increased by lowering the hydrogen/butanedinitrile ratio. © 2001 Academic Press

**Key Words:** nickel–magnesia catalysts; magnesia; succinonitrile; dinitrile; 1,4-butanedinitrile hydrogenation.

## INTRODUCTION

Hydrogenation of nitriles is one of the most widely used methods to obtain amines commercially (1, 2), and production of aliphatic amines has been the most important application. One interesting industrial process is the hydrogenation of 1,6-hexanedinitrile (adiponitrile) to obtain 1,6-hexanediamine which is used as a precursor in the preparation of Nylon-6,6 (3–5).

Recent studies have shown that the hydrogenation–cyclization of dinitriles is a new interesting research field in organic synthesis to obtain N-heterocyclic compounds. Today, pyridine derivatives such as  $\alpha$ - and  $\beta$ -picolines are used to obtain precursors of many chemical products which are important in medicine, farming, and industry. These compounds have usually been prepared by aldol condensation

in the post Prins (6) has recently proposed the catalytic hydrogenation of 2-methylglutaronitrile as an alternative process to obtain these picoline compounds. The 2-methylglutaronitrile is a by-product in the DuPont process for manufacturing adiponitrile from butadiene (6, 7) and, therefore, such a catalytic process means that by-products can be used as raw materials.

Nitrile hydrogenation products are composed mainly of a mixture of primary, secondary, and tertiary amines (8, 9). The condensation reactions between a highly reactive intermediate imine and the primary amine always lead to the formation of such products as secondary and tertiary amines together with the primary amines (10). The selectivity of the nitrile hydrogenation process is of great importance and depends on the properties of the starting nitrile, the catalyst used, and the reaction conditions. However, the catalyst is the most important factor (2, 11). Catalysts based on Co, Ni, and Ru are mostly used to produce primary amines. Cu and Rh catalysts are mostly used to obtain secondary amines while tertiary amines can be prepared by using Pt and Pd catalysts (12, 13).

Amines are usually prepared industrially in the liquid phase at high hydrogen pressures. Nickel catalysts, however, have been used at lower pressures, in the gas phase, although an excess of ammonia was essential to suppress secondary and tertiary amine formation (10, 14). Also, the addition of potassium in dopant amounts enhances the selectivity of nickel catalysts toward primary amines in adiponitrile hydrogenation (15–18). Recently, precursors such as hydrotalcites have made it possible to vary the MgO/Al<sub>2</sub>O<sub>3</sub> ratio and thus control the acidity of the catalysts (19, 20). When this ratio increases, the selectivity to primary amines in the acetonitrile hydrogenation also increases.

Double selective catalysts are required if 6-amino-hexanenitrile is to be obtained selectively in the adiponitrile hydrogenation. Such catalysts lead to primary amines with only one hydrogenated nitrile group. This selectivity could be related to the crystallinity of the active phase. In this respect, Ni/ $\alpha$ -Al<sub>2</sub>O<sub>3</sub> catalysts with nickel particles of

<sup>1</sup> To whom correspondence should be addressed. Fax: +34 977559563. E-mail: [salagre@quimica.urv.es](mailto:salagre@quimica.urv.es)

octahedral morphology (21) and crystalline Raney nickel catalysts (22) have shown very high selectivity to the monoamine compound. It has also been observed that the morphology and size of nickel particles are related to the method used to prepare NiO–MgO systems (23).

In this study, we propose that Ni–MgO systems with nickel metallic phases of different crystallinity can be used to control the selectivity to monoamine or to cyclic derivatives. Different magnesia sources will suppress the condensation reactions and consequently the lifetime of the catalysts will increase. The catalytic tests were performed in the gas phase at 1 atm pressure for the hydrogenation of 1,4-butanedinitrile.

## EXPERIMENTAL

### Catalysts Preparation

NiO of octahedral morphology was prepared according to the method of Estellé (24). It involved thermally decomposing  $\text{Ni}(\text{NO}_3)_2 \cdot 6\text{H}_2\text{O}$  at 373 K for 14 days in order to obtain  $\text{Ni}_3(\text{NO}_3)_2(\text{OH})_4$  as a single phase which was then calcined at 623 K for 40 min to obtain the NiO sample, referred to as NiO. The corresponding catalyst was obtained by reduction under  $\text{H}_2$  at 673 K for 4 h. This sample was named Ni-Oh.

Three NiO–MgO samples were prepared by modifying the MgO source and/or the preparative procedure according to the method previously described (23) which is briefly summarized as follows. The NiO/MgO weight ratio was 4 : 1 for all samples (referred to as 4). Two MgO sources were used: commercial  $\text{MgO}_C$  (BET surface area  $223 \text{ m}^2 \text{ g}^{-1}$ ) and a magnesia obtained by thermal decomposition of magnesium nitrate hexahydrate,  $\text{MgO}_N$  (BET surface area  $2.5 \text{ m}^2 \text{ g}^{-1}$ ), referred to as C and N, respectively.

Two preparative procedures were performed: path A and path B (referred to as subscripts A and B, respectively). Path A involved a direct calcination of a  $\text{Ni}(\text{NO}_3)_2 \cdot 6\text{H}_2\text{O}$  and MgO mixture at 673 K (samples  $4C_A$  and  $4N_A$ ). In path B, a controlled thermolysis of a nickel nitrate and  $\text{MgO}_C$  mixture was carried out to obtain  $\text{Ni}_3(\text{NO}_3)_2(\text{OH})_4$ . This sample was later calcined at a lower temperature (523 K) than in case A (sample  $4C_B$ ).

Finally, all samples obtained by paths A and B were reduced under pure  $\text{H}_2$  at 673 K for 6 h (catalysts  $R4C_A$ ,  $R4N_A$ , and  $R4C_B$ ).

### Air-free Sampling

After the reduction step, the catalysts were always handled under air-free conditions. The samples were transferred in degassed isoctane under a hydrogen atmosphere at room temperature. The isoctane surface-impregnated samples were further isolated from the air either by gold film for the scanning electron microscopy (SEM) study or

by adhesive tape for X-ray diffraction (XRD) monitoring. A glove box was used for mounting. The catalytic activity was measured *in situ*, in the same reactor after reduction, where gas purges, positive gas pressures, and Schlenk techniques were used when necessary.

### BET Surface Areas

Surface areas were calculated from the nitrogen adsorption isotherms at 77 K using a Micromeritics ASAP 2000 surface analyzer and a value of  $0.164 \text{ nm}^2$  for the cross section of the nitrogen molecule.

### X-ray Diffraction (XRD)

Powder X-ray diffraction patterns of the different samples were obtained with a Siemens D5000 diffractometer using nickel-filtered  $\text{Cu K}\alpha$  radiation. Samples were dusted on double-sided adhesive tape and mounted on glass microscope slides. The patterns were recorded over a range of  $2\theta$  angles from  $10^\circ$  to  $90^\circ$  and crystalline phases were identified using the Joint Committee on Powder Diffraction Standards (JCPDS) files.

The XRD patterns of MgO are very similar to those of NiO. The peak positions corresponding to  $2\theta$  angles (with the relative intensities in parentheses), taken from the JCPDS files, are 36.95 (10), 42.91 (100), 62.31 (52), 74.68 (4), and 78.61 (12) for the MgO phase and 37.28 (91), 43.30 (100), 62.92 (57), 75.44 (16) and 79.39 (13) for the NiO phase. Both  $2\theta$  peaks are assigned to the faces (1 1 1), (2 0 0), (2 2 0), (3 1 1), and (2 2 2), respectively. The  $2\theta$  angles and the relative intensities (in parentheses) are 44.51 (100), 51.85 (42), and 76.36 (21) for the Ni phase.

This technique was also used to determine the reduction degree ( $\alpha$ ) of the catalysts by means of the Rietveld method (25). This method implies quantitative phase analysis of multicomponent mixtures from the X-ray powder diffraction data. It is only necessary to know the crystal structure of each phase of interest.

### Temperature-Programmed Reduction (TPR)

Temperature-programmed reduction (TPR) studies were carried out in a Labsys/Setaram TG DTA/DSC thermobalance equipped with a 273–1273 K programmable temperature furnace. The accuracy was  $\pm 1 \mu\text{g}$ .

Each sample (90 mg) was first heated at 423 K in an Ar flow ( $80 \text{ cm}^3/\text{min}$ ) until no change of weight was detected. The sample was then heated in a 5 vol%  $\text{H}_2/\text{Ar}$  flow ( $80 \text{ cm}^3/\text{min}$ ) from 423 K to 1173 K at a rate of  $5 \text{ K min}^{-1}$  and maintained at 1173 K until the reduction process was finished.

### Scanning Electron Microscopy (SEM)

Scanning electron micrographs were obtained with a JEOL JSM6400 scanning microscope operating at an

accelerating voltage in the range 30–35 kV, a work distance (w.d.) between 7–9 mm and at a magnification factor of 40,000 to 50,000.

### Temperature-Programmed Desorption (TPD)

TPD spectra were obtained with a Fisons QTMD 150 gas desorption unit equipped with a 273–1273 K programmable temperature furnace and a mass spectrometer detector.

Samples were reduced in a pure H<sub>2</sub> flow (80 cm<sup>3</sup>/min) from room temperature at 1 K min<sup>-1</sup> up to 673 K. They were isothermally maintained at this last temperature for 4 h to obtain the catalyst Ni-Oh and for 6 h to obtain catalysts R4C<sub>A</sub>, R4C<sub>B</sub>, and R4N<sub>A</sub>. The samples were then cooled to room temperature in the hydrogen flow, evacuated for 1 h at low pressures (<1 Pa), and heated at a rate of 10 K/min up to 1123 K. The hydrogen desorption was detected with the mass spectrometer.

### Hydrogen Chemisorption

Hydrogen chemisorption was measured with a Micromeritics ASAP 2010C instrument equipped with a turbomolecular pump. Samples had been reduced previously under the same conditions under which the catalysts had been prepared. After reduction, the chemisorbed hydrogen was removed in a stream of 30 ml/min of He for 30 min at 683 K. The sample was subsequently cooled to 303 K in the same He stream. The chemisorbed hydrogen was analyzed at 303 K. The nickel surface area was calculated assuming a stoichiometry of one hydrogen molecule per two surface nickel atoms and an atomic cross-sectional area of  $6.49 \times 10^{-20}$  m<sup>2</sup>/Ni atom.

### Determination of the Catalytic Activity

The gas-phase hydrogenation of 1,4-butanedinitrile was studied in a tubular fixed-bed flow reactor heated by an oven equipped with a temperature control system. The reactor was filled with catalyst (500 mg) and the catalytic reaction for 1,4-butanedinitrile vapor at 353 K was measured at 1 atm pressure, using space velocities between 6500–13000 h<sup>-1</sup> and reaction temperatures between 343–453 K.

No diffusional retardation was observed as the residence times lie on the linear portion of the curve obtained when plotting conversion against residence time for different catalyst volumes. Reaction products were analyzed by an on-line HP 5890 gas chromatograph equipped with a 30-m “commercial Rtx-5 amine” capillary column and a flame ionization detector.

Conversion and selectivity were defined by the following equations: conversion (%) = [moles of 1,4-butanedinitrile consumed] × 100/[moles of 1,4-butanedinitrile charged]; selectivity (%) = [moles of one product of reaction] × 100/[moles of 1,4-butanedinitrile consumed]. The carbon mass balance of the process was always maintained.

## RESULTS AND DISCUSSION

### X-Ray Diffraction (XRD)

Sample NiO shows peaks which can be attributed to crystalline NiO whereas the powder diffraction patterns of the NiO–MgO systems (23) show peaks which correspond to a crystalline solid solution of the components.

Table 1 shows the crystalline phases obtained by XRD for the catalysts. The Ni-Oh catalyst contains crystalline nickel as a single phase. However, the reduced catalysts Ni–MgO (samples R4C<sub>A</sub>, R4N<sub>A</sub>, and R4C<sub>B</sub>) have powder diffraction patterns corresponding to two phases: a crystalline solid solution phase and a less crystalline Ni phase (see Table 1). The detection by XRD of a solid solution phase for the catalysts indicates that the reduction of NiO is not complete. Therefore, the presence of magnesia hinders the reduction process, in agreement with what has been reported by Arena *et al.* (26–28).

The degrees of reduction ( $\alpha$ ) were determined from the corresponding diffraction patterns using the Rietveld method (25) for all catalysts (Table 1). The Ni-Oh catalyst had the highest degree of reduction, as expected.

When path A was used to prepare the Ni–MgO catalysts, the degrees of reduction were lower than those when path B was used (0.12 for R4C<sub>A</sub> and 0.29 for R4C<sub>B</sub>) for the same magnesia source. The reduction degree of catalyst R4C<sub>A</sub> is lower because the diffusion between the NiO and MgO phases (which hinders the reduction of NiO) is better at the higher calcination temperature used in path A (673 K) than in path B (523 K).

The reduction degree for catalyst R4N<sub>A</sub> is higher ( $\alpha = 0.56$ ) than that for catalyst R4C<sub>A</sub> ( $\alpha = 0.12$ ). This is in agreement with the diffusion problems observed (23) for the MgO<sub>N</sub> which had larger particles (crystallite sizes >1200 Å) than the MgO<sub>C</sub> (crystallite sizes of 47 Å). TPR results, discussed below, confirm this behavior.

### BET Surface Areas

The surface area of the NiO sample is 11 m<sup>2</sup> g<sup>-1</sup> and those for the NiO–MgO systems range between 24 and 36 m<sup>2</sup> g<sup>-1</sup>. After reduction of the catalytic precursors, a small decrease in surface areas was observed due to the formation of a new

TABLE 1  
Characterization of Catalysts

	Ni-Oh	R4C <sub>A</sub>	R4N <sub>A</sub>	R4C <sub>B</sub>
Crystalline phases (XRD)	Ni	Ni NiO–MgO	Ni NiO–MgO	Ni NiO–MgO
Reduction degree $\alpha$ (XRD) <sup>a</sup>	1	0.12	0.56	0.29
Metallic area <sup>b</sup> (m <sup>2</sup> g <sup>-1</sup> )	0.2	1.6	2.0	4.1

<sup>a</sup> Reduction degree obtained by using the Rietveld method (25).

<sup>b</sup> Metal surface area, calculated from H<sub>2</sub> chemisorption.

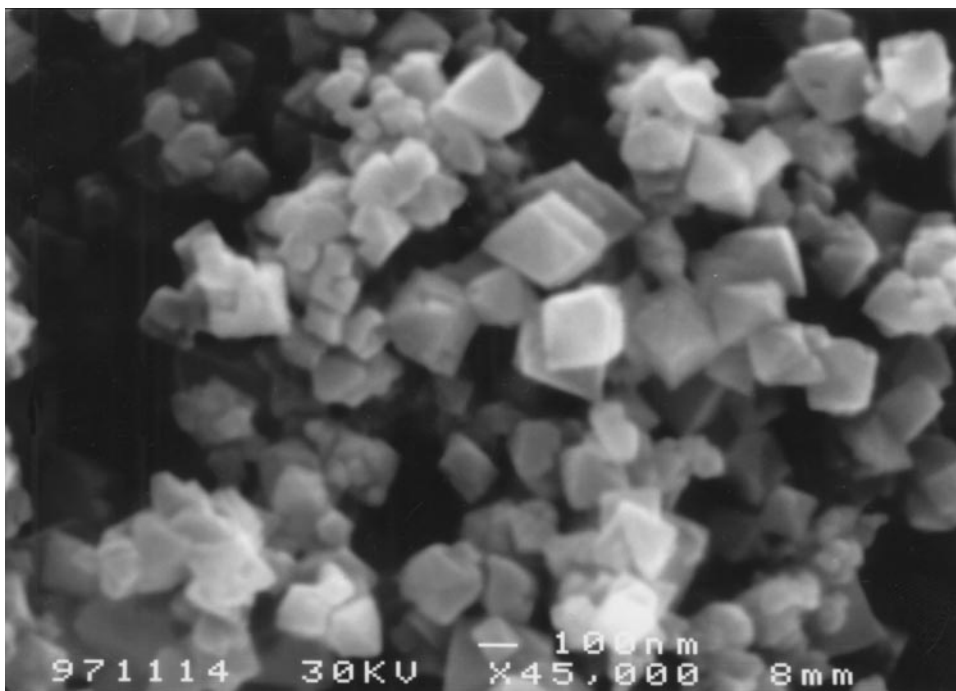


FIG. 1. Scanning electron micrograph of precursor NiO.

crystalline and more compact Ni phase. The low surface areas of the catalysts R4C<sub>A</sub> and R4C<sub>B</sub> (and their catalyst precursors) contrast with the high area of their MgO<sub>C</sub> source (223 m<sup>2</sup> g<sup>-1</sup>). This is in agreement with the results reported by Anderson and Hohlrock (29), who observed considerable sintering of high-surface-area magnesia samples in the presence of low amounts of water vapor at the calcination temperatures used.

#### Temperature-Programmed Reduction (TPR)

The reducibility of the NiO sample was estimated by TPR considering its initial reduction temperature in order to allow comparison with the initial reduction temperature obtained for the NiO–MgO systems previously (23). Our goal in performing these reducibility studies is to confirm the differences in the degrees of reduction ( $\alpha$ ) observed by XRD for the four catalysts, as mentioned above. The initial reduction temperature values ( $T_R$ ) are 583, 598, 604, and 613 K for the samples NiO, 4N<sub>A</sub>, 4C<sub>B</sub>, and 4C<sub>A</sub>, respectively. The initial reduction temperature of the NiO sample (583 K) is lower than that of the systems prepared with magnesia whereas its reduction degree ( $\alpha = 1$ ) is higher (see Table 1). This confirms that the interaction between NiO and MgO leads to the formation of a NiO–MgO solid solution for these systems (27, 28). This hinders the reduction of NiO. Comparing the three Ni–MgO catalysts, the catalyst which has the highest reduction degree (R4N<sub>A</sub>) is the one whose precursor showed the lowest initial reduction temperature.

#### Scanning Electron Microscopy (SEM)

Scanning electron microscopy was used to monitor the morphology and particle size of the different precursors and their reduced forms. Figures 1, 2, and 3 show the micrographs of the NiO, 4C<sub>A</sub>, and 4C<sub>B</sub> samples, respectively.

The NiO sample and its reduced form, Ni–Oh, appear to have the same homogeneous octahedral particles with dimensions around 2500 Å. Therefore, the use of Ni<sub>3</sub>(NO<sub>3</sub>)<sub>2</sub>(OH)<sub>4</sub> as a single precursor of NiO phase becomes a good method to obtain homogeneous octahedral particles in a reproducible way. This is in agreement with what has been reported by Estellé (24).

For the NiO–MgO systems, different paths of preparation lead to samples with different morphologies and particle size distributions. The sample prepared via path B is highly homogeneous and has small particles (around 1000 Å) with non-well-defined octahedral forms. In contrast, the sample prepared via path A has spherical particles between 1000 and 10000 Å. Ni–MgO catalysts do not show significant differences with respect to their catalytic precursors.

#### Temperature-Programmed Desorption (TPD)

To obtain information about their active sites, temperature-programmed desorption of hydrogen was performed for all the catalysts. The mechanisms of adsorption/desorption of hydrogen are extremely complex (30–51), especially when dealing with supported catalysts. This is because phenomena related to the interaction between the

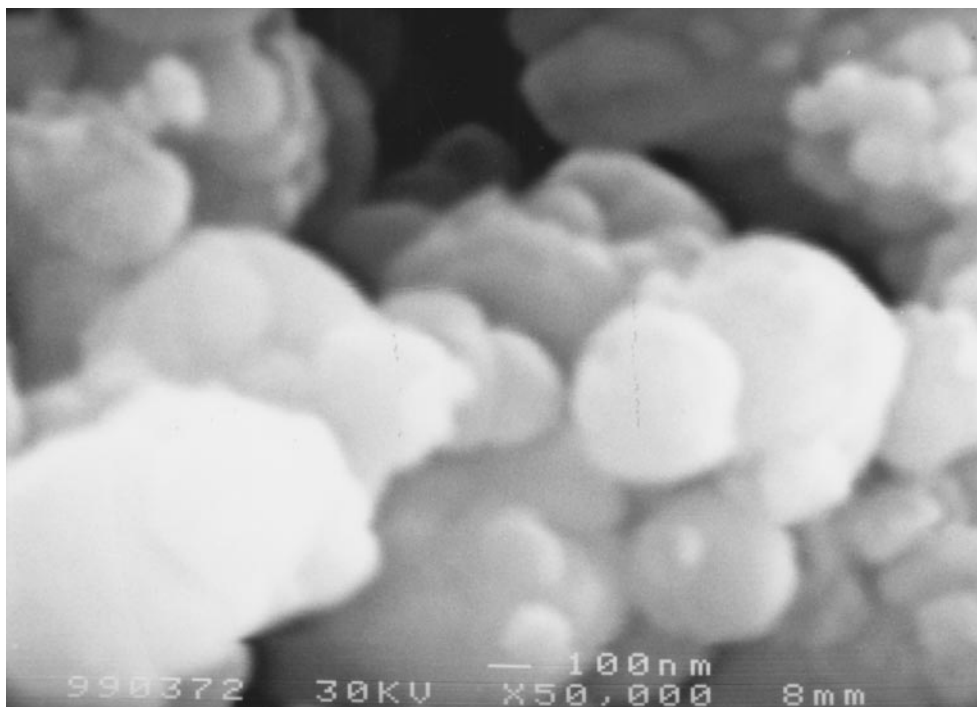


FIG. 2. Scanning electron micrograph of precursor 4C<sub>A</sub>.

active phase and the support can interfere although highly complicated TPD spectra have also been obtained for pure metal catalysts (43). The number and population distribution of adsorbed species depend on many factors: how the catalyst was prepared, the kind of support used, and the

experimental conditions of the measurement such as the weight of the sample examined, the flow rate of the carrier gas, the use of ultrahigh vacuum (UHV), or the shape of the reactor system which affect conditions for removal of desorbed hydrogen.

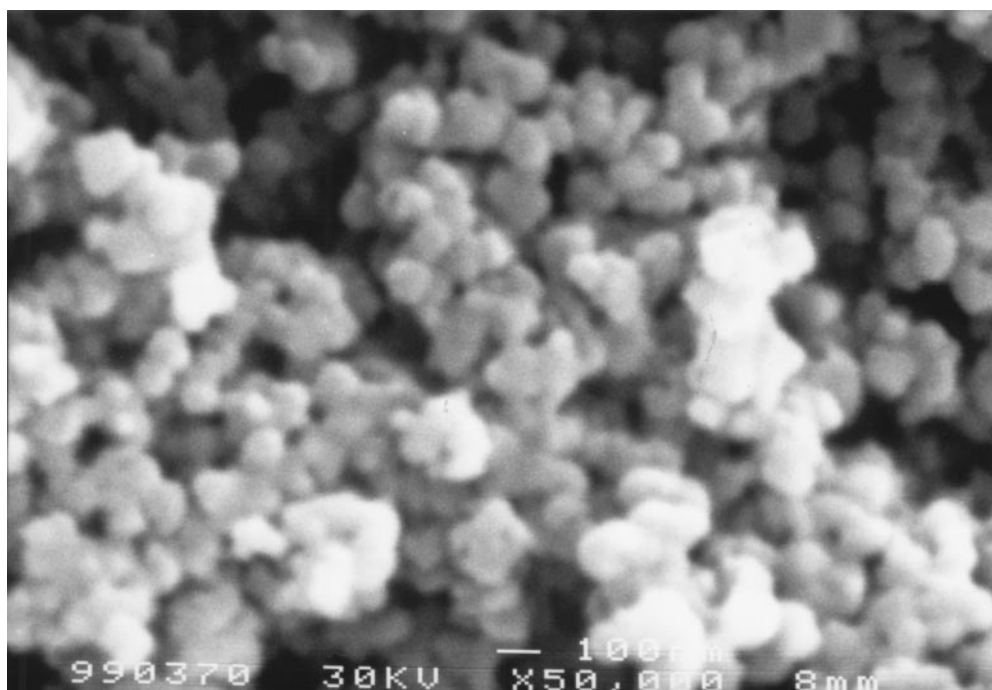


FIG. 3. Scanning electron micrograph of precursor 4C<sub>B</sub>.

TABLE 2

Top Temperatures in the H<sub>2</sub> TPD Spectra for Catalysts Ni-Oh, R4C<sub>A</sub>, R4N<sub>A</sub>, and R4C<sub>B</sub>

Catalysts	Position of peak maxima		
	T <sub>D</sub> < 700 K		T <sub>D</sub> > 700 K
Ni-Oh	476(w)	545(w)	821(w)
R4C <sub>A</sub>	396(m)	600(w)	—
R4N <sub>A</sub>	435(m)	687(s)	811(w)
R4C <sub>B</sub>	450(s)	634(m)	825(w)

Note: s = strong; m = medium; w = weak.

Table 2 summarizes the hydrogen desorption temperature of the peak maxima for catalysts Ni-Oh, R4C<sub>A</sub>, R4N<sub>A</sub>, and R4C<sub>B</sub>. TPD plots show two peaks in the low-temperature region (with maxima at 400–475 K and 545–685 K, respectively) for all catalysts and one peak in the high-temperature region (with maxima at 810–825 K) for catalysts Ni-Oh, R4N<sub>A</sub>, and R4C<sub>B</sub>. The low-temperature region has been associated with different adsorption states of the hydrogen for other nickel catalysts (41, 50, 51). Several authors attribute the occurrence of the high-temperature peaks to hydrogen spillover taking place during high-temperature (above 773 K) treatments of the catalysts (30, 42). Their arguments cannot be applied to the Ni-Oh catalyst which also shows a peak at 821 K. Therefore, a more probable explanation, for all catalysts, is that the high-temperature peak is associated with other adsorption states

of hydrogen (due to a difference in morphology and size of the nickel particles) that we also observed for other nickel catalysts (50, 51).

With all catalysts hydrogen mainly desorbed at low temperatures (<700 K). An important point to emphasize is that H<sub>2</sub> populations of the low-temperature peaks are higher for the systems containing magnesia than for the pure nickel catalyst (Ni-Oh). This may be related to the higher metallic area obtained for the systems with magnesia (see Table 1) and especially to the presence of specific active sites. Therefore, there will be a greater amount of hydrogen available at the reaction temperatures for the Ni-MgO catalysts.

In the reaction mechanisms proposed in the literature for the hydrogenation of dinitrile compounds (8), different reaction products can be obtained if different amounts of hydrogen are consumed. The production of monoamine demands the lowest hydrogen consumption. This fact together with the possibility to correlate the binding strength of the chemisorbed hydrogen with the activity for a specific reaction, as has been reported by some authors (41, 50–52), lead to our interest in the use of TPD results in the interpretation of the catalytic activity.

#### Catalytic Activity

Table 3 shows conversions and selectivities for hydrogenation of 1,4-butanedinitrile on nickel and

TABLE 3

Catalytic Behavior of Four Nickel Catalysts As Influenced by the Space Velocity and the Reaction Temperature

Catalyst	Space velocity (h <sup>-1</sup> )	Reaction temp (K)	Conversion (%)	Selectivity (%)					
				4-Aminobutanenitrile	1,4-Butanediamine	Pyrrolidine	1-Pyrroline	Cracking products	Condensation products
Ni-Oh	6500	473	100	0	1	16	55	0	28
	6500	453	100	9	1	13	52	0	25
	6500	393	100	49	0	0	46	0	5
	9750	403	78	61	0	0	35	0	4
	13000	403	45	77	0	0	20	0	3
R4C <sub>A</sub>	6500	453	100	0	0	71	3	23	3
	13000	453	100	0	0	76	18	5	1
	13000	403	100	4	16	30	46	0	4
	13000	383	99	16	23	36	23	0	2
	13000	353	84	56	7	0	32	0	5
R4N <sub>A</sub>	6500	453	100	0	0	36	0	64	0
	6500	433	100	0	0	59	20	21	0
	13000	403	100	23	17	7	53	0	0
	13000	383	100	60	18	0	20	0	0
	13000	363	93	68	0	0	28	0	0
R4C <sub>B</sub>	6500	453	100	0	0	0	0	100	0
	6500	423	100	0	0	72	0	28	0
	6500	363	100	19	15	0	66	0	0
	13000	403	100	41	0	0	56	0	3
	13000	343	100	85	0	0	12	0	3

nickel-magnesia catalysts (Ni-Oh, R4C<sub>A</sub>, R4N<sub>A</sub>, R4C<sub>B</sub>) under the conditions given in the Experimental section.

The activity of the two pure magnesia samples was also tested and they were shown to be catalytically inactive under the reaction conditions studied.

As Table 3 shows, the reaction products were 4-aminobutanenitrile, 1,4-butanediamine, pyrrolidine, 1-pyrroline, and cracking and condensation species. The selectivities toward these reaction products depend on the catalyst used. This dependence has been studied by optimizing the reaction conditions (reaction temperature, space velocity, and H<sub>2</sub>/dinitrile ratio).

High-molecular-weight products are obtained in higher amounts when the catalyst is used without magnesia (Ni-Oh) at a low space velocity (6500 h<sup>-1</sup>) and at high temperatures (473–453 K). On the other hand, nickel-magnesia catalysts hardly produce any condensation products and consequently they do not undergo catalyst deactivation. This is probably a consequence of the basic character of magnesia which favors the elimination of amines and prevents secondary reactions. These condensation products have been described by Prins (6) as dimers obtained as a result of an intermolecular amine-imine condensation reaction. However, if these basic catalysts are used at low space velocity (6500 h<sup>-1</sup>) and high temperatures (453–423 K), cracking products are obtained. The catalyst which provides most cracking products is the one with the highest metallic area, R4C<sub>B</sub> (see Table 1), and the highest amount of hydrogen desorbed at the reaction temperatures studied

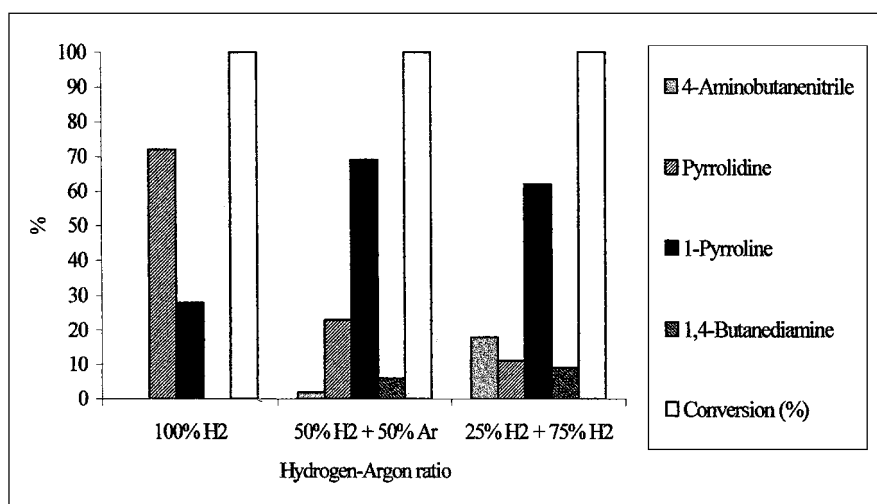
(453–343 K). This catalyst is the most active (100% conversion) at all temperatures and space velocities used.

*Formation of 4-aminobutanenitrile and 1,4-butanediamine.* All the catalysts showed low selectivities toward 1,4-butanediamine. The Ni-Oh catalyst hardly produces any of this diamine while the selectivity to the monoamine, 4-aminobutanenitrile (77%), is highest at the lowest conversion value (45%), working at a space velocity of 13,000 h<sup>-1</sup> and a reaction temperature of 403 K.

However, the basic Ni-MgO catalysts produced low amounts of the diamine (selectivity <24%) and conversions and selectivities toward 4-aminobutanenitrile were high. The most active (100%) and selective catalyst to 4-aminobutanenitrile (85%) was type R4C<sub>B</sub>. This result was obtained when working at the same space velocity as with the NiOh catalyst but at a lower reaction temperature (343 K).

The main difference between the two types of systems is their activity: the Ni-MgO catalysts are more active than the Ni-Oh. This means that the nickel-magnesia systems can be used at lower reaction temperatures in which cyclization is not favored. This kind of catalysts makes it possible to increase the selectivity to monoamine without a significant loss of conversion.

The fact that the highest activity was found for catalyst R4C<sub>B</sub> at 343 K is probably related to the presence of one intense hydrogen TPD peak with a maximum at 450 K (see Table 2). This provides enough desorbed hydrogen at this



\* All experiments have been obtained at 423 K reaction temperature and at a space velocity of 6500 h<sup>-1</sup>.

FIG. 4. Product selectivities for the hydrogenation of 1,4-butanedinitrile on R4C<sub>B</sub> catalyst as a function of the hydrogen/1,4-butanedinitrile ratio. (The modification of these ratios has been realized by diluting hydrogen with argon.)

reaction temperature for the monoamine to be selectively obtained with high conversion values (100%).

The Ni-Oh catalyst probably has a lower activity because there is less hydrogen available at lower reaction temperatures (catalyst Ni-Oh has a weak desorption peak with a maximum at 476 K) and additionally it is partially deactivated by the condensation products generated, as mentioned above.

In a previous study (21), the selective hydrogenation of one nitrile group was related to the presence of a considerable number of octahedral crystal sites. Our experiments have confirmed this since no diamine was observed when the nickel catalyst (Ni-Oh) was used. In contrast, the Ni-MgO catalysts may provide diamine as a minor product because the nickel particles do not show well-defined faces, as observed by SEM and as confirmed by XRD.

**Formation of pyrrolidine and 1-pyrroline.** The Ni-Oh catalyst shows low selectivities to pyrrolidine. The highest value (16%) was obtained by working at 473 K and a space velocity of 6500 h<sup>-1</sup> at 100% conversion. All Ni-MgO systems provide higher selectivities to pyrrolidine than the Ni-Oh catalyst. Catalyst R4C<sub>A</sub> has a 76% selectivity at 453 K and 13,000 h<sup>-1</sup> and catalyst R4C<sub>B</sub> has a 72% selectivity at 423 K and 6500 h<sup>-1</sup> for a 100% of conversion for both catalysts.

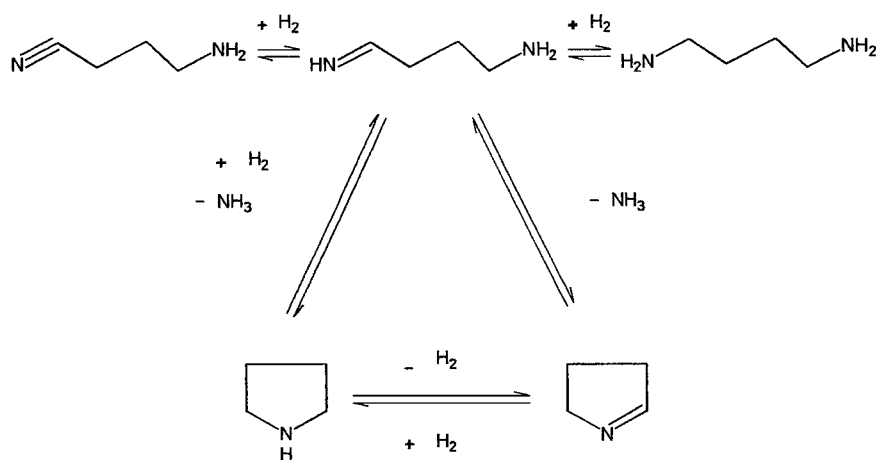
The Ni-Oh catalyst shows the highest selectivity to 1-pyrroline (55%) at the highest reaction temperature tested (473 K) and at a space velocity of 6500 h<sup>-1</sup> for a 100% conversion. However, catalysts containing magnesia show the highest 1-pyrroline selectivities between 46–66% at a conversion of 100% at lower reaction temperatures (363 and 403 K). The most active catalyst, R4C<sub>B</sub>, gave the highest selectivity to 1-pyrroline, 66% at 363 K, whereas R4C<sub>A</sub> and R4N<sub>A</sub>, which are less active, gave the highest values to 1-pyrroline (46% and 53%, respectively) at 403 K. For these catalysts, at lower temperature the amount of

hydrogen available probably decreases, and consequently the formation of the less hydrogenated species, monoamine, increases.

Pyrrolidine and 1-pyrroline are amine and imine cyclic compounds, respectively. The formation of the imine probably needs lower amounts of hydrogen if both products are obtained from the same intermediate compound (4-aminobutaneimine). In order to investigate how hydrogen influences the production of pyrrolidine and 1-pyrroline, several experiments were performed with catalyst R4C<sub>B</sub>, varying the H<sub>2</sub>/1,4-butanedinitrile ratio and maintaining the same total flow (by dilution with argon) at a temperature of 423 K and a space velocity of 6500 h<sup>-1</sup>. The results are shown in Fig. 4.

When 100% H<sub>2</sub> was used, the selectivity to pyrrolidine was high (72%); when hydrogen was diluted with 50% Ar, the selectivity to 1-pyrroline clearly increased (69%). Nevertheless, a further decrease in the amount of hydrogen in the total flow (25% H<sub>2</sub>, 75% Ar) did not significantly change the selectivity to 1-pyrroline but there was an increase in the selectivity to 4-aminobutanenitrile (18%).

These results enabled us to propose Scheme 1 which could explain the relative formation of 1-pyrroline, pyrrolidine, and 4-aminobutanenitrile as a function of the availability of hydrogen under the reaction conditions. Once the aminoimine intermediate has been obtained, there are two possible side reactions: a ring closure of the intermediate with loss of ammonia and uptake of one H<sub>2</sub> and a ring closure with the loss of ammonia only. The second side reaction is probably only possible if the proportion of hydrogen in the total flow is decreased. It is of considerable importance that 4-aminobutanenitrile appeared at the lowest H<sub>2</sub>/Ar ratio amount (see Fig. 4). Hence, when less hydrogen is available, a higher selectivity to 1-pyrroline will be found. Finally, under more diluted conditions more 4-aminobutanenitrile will be formed, even at high reaction temperatures.



**Scheme 1.** Pyrrolidine and 1-pyrroline obtained by catalytic hydrogenation of 1,4-butanedinitrile (succinonitrile).

## CONCLUSIONS

Several nickel–magnesia catalysts have been prepared by varying the magnesia source and the preparative method. Their performance has been compared with the behavior of a nickel catalyst of octahedral morphology in the hydrogenation of 1,4-butanedinitrile. All samples were structurally characterized by the application of BET, XRD, TPR, SEM, H<sub>2</sub> chemisorption, and TPD techniques. XRD was used to identify the solid solutions obtained for all the NiO–MgO catalyst precursors and the catalysts. The Ni–Oh catalyst contained nickel-only crystalline phase and all the Ni–MgO catalysts consisted of Ni and a NiO–MgO solid solution. XRD combined with TPR enabled us to establish the sequence of reducibility of the catalyst precursors: NiO > 4N<sub>A</sub> > 4C<sub>B</sub> > 4C<sub>A</sub>.

SEM showed homogeneous octahedral crystallites for the Ni–Oh catalyst, whereas the micrographs obtained for the systems containing magnesia showed nickel particles with non-well-defined faces, the homogeneity and sizes of which depended on the preparative path used. The NiO–MgO prepared by path B gave rise to a homogeneous system with particle sizes of around 1000 Å.

The Ni–MgO catalysts showed higher activities than the Ni–Oh catalyst. This may be due to their higher metal surface areas and hence the greater amount of available chemisorbed hydrogen (H<sub>2</sub> TPD results). R4C<sub>B</sub> was the most active catalyst under all the reaction conditions studied. This is because its metal surface area was the highest (4.1 m<sup>2</sup> g<sup>-1</sup>) as was its population of weakly bound H<sub>2</sub>.

In the nickel–magnesia catalysts, the presence of MgO suppresses the condensation reactions and consequently there is no catalyst deactivation, probably due to the basic character of magnesia which favors the elimination of amines and prevents secondary reactions.

The selectivity toward cyclic products (pyrrolidine and 1-pyrroline) can be modified by controlling the space velocity, the reaction temperature, and the hydrogen/adiponitrile ratio. High temperatures and low space velocities were required in order to obtain pyrrolidine. A decrease in the hydrogen/1,4-butanedinitrile ratio involves an increase in the selectivity to 1-pyrroline.

Diamine was absent in the product stream when the Ni–Oh catalyst was used but it was detected as a minor product when the Ni–MgO catalysts were used. This may be due to the higher crystallinity of the nickel phase in the Ni–Oh catalyst.

Catalyst R4C<sub>B</sub> shows the highest selectivity to 4-aminobutanenitrile (85%). This has to be ascribed to the characteristic surface properties of this catalyst, leading to a sufficient coverage with weakly bound hydrogen which permits the choice of lower reaction temperatures. At these lower temperatures, cyclization is not favored and the amount of hydrogen available could produce monoamine

selectively. If the reaction temperature is decreased and/or the hydrogen/adiponitrile ratio is decreased to a large extent, the monoamine selectivity increases.

## REFERENCES

- Weissermel, K., and Arpe, H. J., "Industrial Organic Chemistry." Verlag Chemie, Berlin, 1978.
- Volf, J., and Pasek, J., in "Catalytic Hydrogenation, Studies in Surface Science and Catalysis" (L. Cervený, Ed.), Vol. 27. Elsevier, Amsterdam, 1986.
- Lazaris, A. Y., Zilberman, E. N., Lunicheva, E. V., and Vedin, A. M., *Zh. Prikl. Khim.* **38**, 1097 (1965).
- Bolle, J., French Patent 2 063378, 1971.
- Medina, F., Salagre, P., Sueiras, J. E., and Fierro, J. L. G., *J. Mol. Catal.* **68**, L17 (1991).
- Prins, R., *Catal. Today* **37**, 103 (1997).
- Harrison, C. R., in "Catalysis and Chemical Processes" (R. Pearce and W. R. Patterson, Eds.), Chapter 7. 1981.
- Mares, F., Galle, J. E., Diamond, S. E., and Regina, F. J., *J. Catal.* **112**, 145 (1988).
- Huang, Y., and Sachtler, W. M. H., *Appl. Catal. A: Gen.* **182**, 365 (1999).
- Augustine, R. L., *Catal. Rev.* **13**, 285 (1976).
- Frank, G., and Neubauer, G., German Patent 3 402734 A1, 1984 (BASF A.G.).
- Greenfield, H., *Ind. Eng. Chem. Prod. Res. Dev.* **6**, 142 (1967).
- Pasek, J., Kostova, N., and Dvorak, B., *Collect. Czech. Chem. Commun.* **46**, 1011 (1981).
- Schowogler, E. J., and Adkins, H., *J. Am. Chem. Soc.* **61**, 3449 (1939).
- Medina, F., Salagre, P., Sueiras, J. E., and Fierro, J. L. G., *Appl. Catal. A: Gen.* **92**, 131 (1992).
- Medina, F., Salagre, P., Sueiras, J. E., and Fierro, J. L. G., *Solid State Ionics* **59**, 205 (1993).
- Medina, F., Salagre, P., Sueiras, J. E., and Fierro, J. L. G., *Appl. Catal. A: Gen.* **99**, 115 (1993).
- Medina, F., Salagre, P., Sueiras, J. E., and Fierro, J. L. G., *J. Chem. Soc., Faraday Trans.* **90**(10), 1455 (1994).
- Medina, F., Dutartre, R., Tichit, D., Coq, B., Dung, N. T., Salagre, P., and Sueiras, J. E., *J. Mol. Catal. A: Chem.* **119**, 201 (1997).
- Dung, N. T., Tichit, D., Chiche, B. H., and Coq, B., *Appl. Catal. A: Gen.* **169**, 179 (1998).
- Medina, F., Salagre, P., Sueiras, J. E., and Fierro, J. L. G., *J. Chem. Soc., Faraday Trans.* **89**(21), 3981 (1993).
- Yu, X., Li, H., and Deng, J. F., *Appl. Catal. A: Gen.* **199**, 191 (2000).
- Serra, M., Salagre, P., Cesteros, Y., Medina, F., and Sueiras, J. E., *Solid State Ionics* **134**, 229 (2000).
- Estellé, J., Ph.D. thesis, Rovira i Virgili University, Tarragona, Spain, 1998.
- Bish, D. L., and Howard, S. A., *J. Appl. Crystallogr.* **21**, 86 (1988).
- Arena, F., Frusteri, F., Parmaliana, A., Plyasova, L., and Shmakov, A. N., *J. Chem. Soc., Faraday Trans.* **92**, 469 (1996).
- Parmaliana, A., Arena, F., Frusteri, F., and Giordano, N., *J. Chem. Soc., Faraday Trans.* **86**(14), 2663 (1990).
- Arena, F., Frusteri, F., and Parmaliana, A., *Appl. Catal. A: Gen.* **187**, 127 (1999).
- Anderson, P. J., and Hohlrock, R. F., *Trans. Faraday Soc.* **58**, 1993 (1962).
- Páal, Z., and Menon, P. G., *Catal. Rev.-Sci. Eng.* **25**(2), 229 (1983).
- "Hydrogen Effects in Catalysis" Z. Páal and P. G. Menon, Eds., Marcel Dekker, New York, 1988.
- Falconer, J. L., and Schwarz, J. A., *Catal. Rev.-Sci. Eng.* **25**, 141 (1983).
- Raupp, G. B., and Dumesic, J. A., *J. Catal.* **95**, 587 (1985).
- Raupp, G. B., and Dumesic, J. A., *J. Catal.* **97**, 85 (1986).

35. Arai, M., Nishiyama, Y., Masuda, T., and Hashimoto, K., *Appl. Surf. Sci.* **89**, 11 (1995).
36. Ferreira-Aparicio, P., Guerrero-Ruiz, A., and Rodriguez-Ramos, I., *J. Chem. Soc., Faraday Trans.* **93**(19), 3563 (1997).
37. Popova, N. M., Babenkova, L. V., and Sokol'skii, D. V., *Kinet. Katal.* **10**(5), 1177 (1969).
38. Bartholomew, C. H., *Catal. Lett.* **7**, 27 (1990).
39. Lee, P. I., and Schwartz, J. A., *J. Catal.* **73**, 272 (1982).
40. Zielinski, J., *Polish J. Chem.* **69**, 1187 (1995).
41. Smeds, S., Salmi, T., Lindfors, L. P., and Krause, O., *Appl. Catal. A: Gen.* **144**, 177 (1996).
42. Kramer, P., and Andre, M., *J. Catal.* **58**, 287 (1979).
43. Konvalinka, J. A., Van Oeffelt, P. H., and Scholten, J. J. F., *Appl. Catal.* **1**, 141 (1981).
44. Weatherbee, G. D., and Bartholomew, C. H., *J. Catal.* **87**, 55 (1984).
45. Spinicci, R., and Tofanari, A., *React. Kinet. Catal. Lett.* **27**, 65 (1985).
46. Ikushima, Y., Arai, M., and Nishiyama, Y., *Appl. Catal.* **11**, 305 (1984).
47. Glugla, P. G., Bailey, K. M., and Falconer, J. L., *J. Catal.* **115**, 24 (1989).
48. Rankin, J. L., and Bartholomew, C. H., *J. Catal.* **100**, 533 (1986).
49. Stockwell, D. M., Bertuccio, A., Coulston, G. W., and Bennet, C. O., *J. Catal.* **113**, 317 (1988).
50. Cesteros, Y., Salagre, P., Medina, F., and Sueiras, J. E., *Appl. Catal. B: Environ.* **25**, 213 (2000).
51. Cesteros, Y., Salagre, P., Medina, F., and Sueiras, J. E., *Appl. Catal. B: Environ.* **22**, 135 (1999).
52. Marécot, P., Paraiso, E., Dumas, J. M., and Barbier, J., *Appl. Catal.* **74**, 261 (1991).